

Self-Correction Inside the Model: Leveraging Layer Attention to Mitigate Hallucinations in Large Vision–Language Models

April Fu
Independent Researcher
fq.april@gmail.com

Abstract

Although Large Vision-Language Models (LVLMs) have made substantial progress, hallucination, where generated text is not grounded in the visual input, remains a challenge. As LVLMs become stronger, previously reported hallucination patterns, such as linguistic bias and “overthinking” phenomenon, become far less consistent, making the corresponding mitigation techniques substantially less effective. In this paper, we introduce an *Internal self-Correction mechanism utilizing Layer Attention (ICLA)* that operates directly on hidden states during generation. Each layer selectively retrieves information from all preceding layers through a diagonal cross-layer attention mechanism, enabling self-refinement without any external correction signals. With introducing and training only 0.2M and 0.1M additional parameters on LLaVA1.5-7B and Qwen2.5-VL-7B, ICLA consistently improves visual grounding across multiple hallucination benchmarks, demonstrating its effectiveness for more advanced LVLMs.

1. Introduction

Large Vision-Language Models (LVLMs) [1, 19, 25, 28, 48] have significantly advanced the capabilities of multimodal learning in broad tasks that require joint reasoning over textual and visual information, including image captioning and visual question answering (VQA) [8, 10, 24, 42]. Despite these advancements, hallucination remains a persistent challenge in most LVLMs. This phenomenon refers to cases where the generated text is not grounded in the visual input, often describing objects, or relationships that do not exist in the image [20, 45].

Several studies have investigated the causes of hallucination in LVLMs. One major factor is modality imbalance, where the model tends to over-rely on linguistic priors while underutilizing visual evidence—particularly when images are ambiguous, cluttered, or lack informative content [21, 36, 45, 47]. In addition, LVLMs often exhibit a

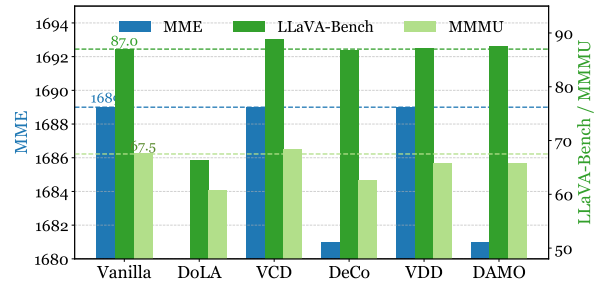


Figure 1. Performance degradation of existing methods on Qwen2.5-VL-7B, where DoLA exhibits a significant drop, while the performance drop of MME exceeds the plot range and is not shown in the figure.

phenomenon termed as “overthinking”, in which the model captures the correct information in early layers but progressively suppresses visual cues in deeper layers. This over-processing can inadvertently give rise to hallucinated content during text generation [4, 5, 20, 35].

Many approaches have been proposed to address this limitation. Training-based methods aim to enhance grounding by leveraging supervised fine-tuning (SFT) or reinforcement learning from human feedback (RLHF) on high-quality data [21, 36]. Prompt engineering strategies, such as self-correction [17, 39] and self-consistency [3, 38], further improve model reliability by iteratively refining outputs or aggregating multiple generations to reduce hallucinations. More recently, contrastive decoding (CD) has emerged as an effective strategy, improving grounding by first generating referring logits conditioned on hallucinated visual or textual inputs, and then contrasting the hallucinated logits from the logits with normal input to obtain the final logits [18, 27, 29, 32, 37, 45–47]. In addition, several studies have sought to mitigate the “overthinking” phenomenon through accumulative decoding (AD), which propagates information from earlier layers that retain visual semantics to later layers, thereby reducing the emergence of hallucinated content [4, 33, 35, 41].

However, with the advancement of training strategies and the availability of high-quality multimodal data, we find that these previously observed hallucination patterns, such as over-reliance on linguistic priors and the “overthinking” phenomenon, are no longer clearly present in recent LVLMs. Through an in-depth analysis of a large number of erroneous cases from Qwen2.5-VL-7B [2], including the inspection of its internal probability dynamics during inference, we observe *no consistent or significant hallucination trends* as reported in earlier works. Moreover, as shown in Figure 1, when evaluating representative methods designed to mitigate these issues on Qwen2.5-VL-7B, we observe that most of them lead to a noticeable performance drop, while only a few perform comparably to the vanilla model, bringing no observable improvements overall.

These observations motivate us to design a more adaptive and scalable paradigm for hallucination mitigation in modern advanced LVLMs, independent of any specific hallucination pattern. In this paper, we propose an **I**nternal **s**elf-**C**orrection mechanism utilizing **L**ayer **A**ttention (**I**CLA) that operates within the model’s hidden states during generation. Specifically, each layer can actively retrieve information from all preceding layers, self-correcting its hidden state representation according to its current context, thereby mitigating potential hallucinations iteratively. We formulate this process as a cross-layer attention operation, where the hidden state of the current layer serves as the query, and those from all preceding layers serve as keys and values. This design makes **I**CLA particularly suitable for addressing hallucinations in more advanced models where no clear patterns are observable.

Furthermore, to prevent information leakage and cross-position contamination, we apply a diagonal attention mask along the token dimension, ensuring that each hidden state at the current layer can only attend to the hidden states of the same position from all preceding layers, and not to any hidden state of other positions. The aggregated cross-layer attention output information is then integrated back into the hidden state of current layer, refining its representation and reinforcing visual grounding.

We apply **I**CLA on LLaVA1.5-7B and Qwen2.5-VL-7B, where most prior hallucination patterns and method evaluations were conducted on LLaVA1.5-7B, and Qwen2.5-VL-7B represents a more advanced LVLm. By introducing and training only 0.2M and 0.1M additional parameters on LLaVA1.5-7B and Qwen2.5-VL-7B, respectively, **I**CLA achieves strong performance across multiple hallucination benchmarks on both models, demonstrating its effectiveness in mitigating hallucinations. Notably, **I**CLA attains excellent results on Qwen2.5-VL-7B, further highlighting its suitability for complex and advanced LVLms. The main contributions of this paper are summarized as follows:

- We reveal that previously observed hallucination patterns

and corresponding mitigation methods are no longer effective for more advanced LVLms.

- We propose **I**CLA, an internal self-correction mechanism utilizing layer attention, in which each hidden state can adaptively retrieve information from preceding layers and refine itself accordingly.
- Extensive experiments on LLaVA1.5-7B and Qwen2.5-VL-7B demonstrate the effectiveness of **I**CLA. Notably, **I**CLA achieves state-of-the-art performance on Qwen2.5-VL-7B, highlighting its suitability for complex and advanced LVLms.

2. Related Work

2.1. Causes of Hallucination in LVLms

Modality Imbalance. Modality imbalance refers to the tendency of LVLms to over-rely on language priors while underutilizing visual information [11, 12, 16, 22, 31, 37]. This issue primarily stems from the model architecture, where a visual encoder is typically connected to a pre-trained large language model (LLM). As a result, the linguistic component often dominates multimodal reasoning. For instance, VCD [45] attributes hallucinations to the strong statistical biases inherent in language models, particularly when visual cues are weak or ambiguous. Similarly, IBD [47] observes that LVLms tend to overlook fine-grained visual details, producing linguistically plausible but visually ungrounded responses.

“Overthinking”. Beyond modality imbalance, LVLms also tend to “overthink” [4, 33, 35, 41], a phenomenon where the model initially infers the correct information but subsequently modifies or overrides it in later layers. For example, DeCo [4] finds that visual features captured in early layers are progressively suppressed in deeper layers, weakening visual grounding. DAMO [35] further demonstrates that, although LVLms encode accurate visual cues, unstable activations in later layers reduce the probabilities of correct tokens, leading to hallucinations. Similarly, DCLA [33] confirms this trend, showing that hallucinations primarily emerge during the later decoding stages, consistent with DAMO’s findings.

2.2. Methods of Hallucination Mitigation in LVLms

Training-based Methods. Training-based approaches aim to improve visual grounding by fine-tuning LVLms on high-quality data or leveraging reinforcement learning from human feedback (RLHF) [5, 9, 13, 21, 36, 37, 40]. For instance, RLHF-V [36] and POVID [21] construct pairs of hallucinated and non-hallucinated outputs to fine-tune models via Direct Preference Optimization (DPO) algorithm [30], penalizing hallucinated generations. HIO [40], on the other hand, employs a contrastive loss to help the

model distinguish grounded visual context from hallucinated text, thereby reinforcing alignment between visual inputs and generated outputs.

Non-Training-based Methods. Since training-based methods require substantial computational resources and high-quality curated data for fine-tuning, non-training-based methods have recently gained increasing attention for hallucination mitigation. These approaches primarily focus on analyzing and leveraging the internal probability dynamics of LVLMs to reduce hallucinations. For example, contrastive decoding (CD) contrasts logits between original and perturbed visual or textual inputs to alleviate hallucinations by reducing the model’s over-reliance on linguistic priors [15, 18, 26, 27, 29, 32, 37, 44–47]. In addition, to address the “overthinking” limitation, accumulative decoding (AD) has been proposed. AD operates on the hidden states during generation in an accumulative manner, complementing visual information from earlier layers to later ones, thereby preserving visual grounding and mitigating the suppression of visual cues in deeper layers [4, 33, 35, 41].

2.3. Layer Attention

Layer attention has been explored in earlier studies on deep convolutional neural networks (DCNNs) as a way to improve information flow across depth. For instance, DIANet [14] employs a shared LSTM to capture inter-layer dependencies, and subsequent works [6, 7, 34] further develop more sophisticated mechanisms for propagating and refining information across layers. These approaches, although primarily designed for smaller models and general feature enhancement, provide valuable insight into the benefits of cross-layer communication. Inspired by this line of research, our work revisits cross-layer interaction in the context of LVLMs, leveraging it for adaptive refinement, thereby iteratively mitigating hallucination.

3. Method

We begin by reviewing the information flow in LVLMs to highlight the transformation of hidden states. Subsequently, we introduce the overall architecture of our proposed Internal Self-Correction via Layer Attention (ICLA) in detail. Finally, we elaborate the Cross-Layer Attention (CLA) module, which is the key component in ICLA.

3.1. Preliminaries

LVLMs process multimodal inputs through a stack of transformer layers that iteratively refine token representations. Let the multimodal input be $x = (x_1, \dots, x_T)$, where each x_i denotes either a visual or textual token embedding. The

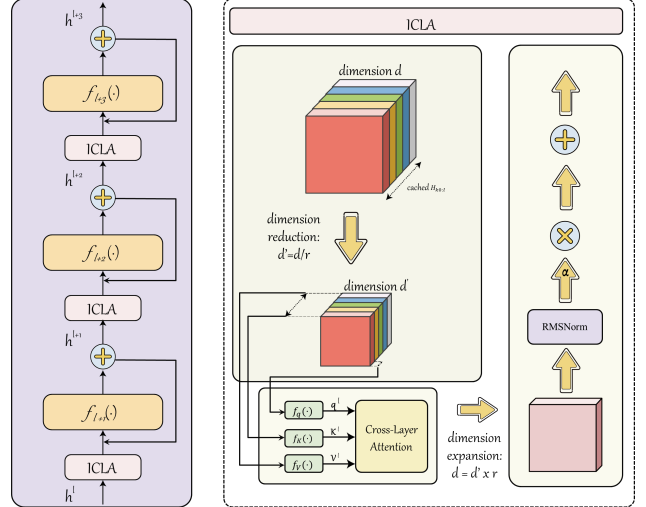


Figure 2. Overall architecture of ICLA.

model maintains a sequence of hidden states across L layers, defined as:

$$h^l = (h_1^l, \dots, h_T^l), \quad l = 0, \dots, L, \quad (1)$$

where $h_i^l \in \mathbb{R}^d$ represents the hidden state of token x_i at the l -th layer, and d denotes the dimensionality of the hidden states. By definition, the initial hidden state h^0 corresponds to the input embeddings x .

Within the model, the hidden states are iteratively updated through transformer layers along with the residual connection:

$$h^{l+1} = f_{l+1}(h^l) + h^l, \quad (2)$$

where $f_{l+1}(\cdot)$ denotes the transformation function of the $(l + 1)$ -th layer, typically consisting of multi-head self-attention and feed-forward submodules. For brevity, we omit the normalization here. After the final layer, the hidden states h^L are used to predict the next-token distribution:

$$P(y_t | x, y_{<t}) = \text{Softmax}(W_o \cdot h_t^L), \quad (3)$$

where h_t^L is the final-layer hidden state of the t -th token, W_o is the output projection matrix.

3.2. Internal Self-Correction via Layer Attention

To address hallucinations in advanced LVLMs, where previously observed patterns and mitigation strategies fail to generalize, we propose ICLA, which enables each hidden state to adaptively retrieve informative representations from preceding layers, thereby dynamically and iteratively refining its own representation and self-correcting the potential hallucinations. The overall architecture of ICLA is shown in Figure 2.

Specifically, at the l -th layer, we first store the hidden states from the k_0 -th to the l -th layer, forming a hidden state cache for the subsequent cross-layer attention mechanism:

$$H_{k_0:l} = \{h^k\}_{k=k_0}^l \in \mathbb{R}^{(l-k_0+1) \times T \times d}, \quad (4)$$

where k_0 serves as the starting layer for hidden state refinement as modifying early layers may destroy the normal inference context [33, 35, 41]. After obtaining the hidden state cache, cross-layer attention is applied to retrieve relevant information from previous layers:

$$O^l = \text{CLA}(H_{k_0:l}), \quad (5)$$

where CLA denotes the cross-layer attention module (detailed in Section 3.3) and $O^l \in \mathbb{R}^{T \times d}$ represents the attention output. Finally, the attention output is scaled and used to refine the current hidden states:

$$h^l := h^l + \alpha \cdot \text{RMSNORM}(O^l), \quad (6)$$

where α is the scaling factor controlling the refinement strength. Here, RMSNorm refers to root mean square normalization, which normalizes the hidden state along the feature dimension to stabilize training and preserve the scale of activations. Then the refined hidden states h^l are used to compute the next layer’s hidden states h^{l+1} for iterative update according to Equation 2.

3.3. Cross-Layer Attention

In this section, we describe the Cross-Layer Attention (CLA) module, which differs from standard self-attention and cross-attention by processing information across transformer layers rather than within a single layer or modality.

Given the hidden state cache $H_{k_0:l}$, we first compute the query, key, and value projections as follows:

$$\begin{cases} q^l = W_q \cdot h^l \\ K^l = W_K \cdot H_{k_0:l} \\ V^l = W_V \cdot H_{k_0:l}, \end{cases} \quad (7)$$

where h^l is the last element in $H_{k_0:l}$, representing the current hidden state. W_q , W_K , and W_V are learnable linear layers with a bottleneck: we first reduce the hidden dimension from d to latent hidden dimension $d' = d/r$ for improving training and inference efficiency and r serves as the reduction ratio, similar to [14, 34].

Then, the obtained query, key, and value are used to compute the attention output. To ensure that each token at the i -th position in the current l -th layer only attends to representations from previous layers at the same i -th position, we extract the diagonal of the attention matrix over the token dimension:

Algorithm 1: Internal Self-Correction via Layer Attention (ICLA)

Input: Multimodal input $x = (x_1, \dots, x_T)$; total layers L

Output: Refined hidden states h^L

```

1 Initialization:  $h^0 \leftarrow x$ ; // Input embeddings
2 for  $l = 1$  to  $L$  do
3    $h^l \leftarrow f_l(h^{l-1}) + h^{l-1}$ ; // Standard transformer update
4   if  $l > k_0$  then
5      $H_{k_0:l} = \{h^k\}_{k=k_0}^l$ ; // Cache recent hidden states
6     Cross-Layer Attention:
7        $q^l = W_q \cdot h^l$ ,  $K^l = W_K \cdot H_{k_0:l}$ ,
8        $V^l = W_V \cdot H_{k_0:l}$ 
9        $\alpha^l = \text{diag}\left(\text{softmax}\left(\frac{q^l \cdot (K^l)^\top}{\sqrt{d'}}\right)\right)$ 
10       $O^l = W_{\text{out}} \cdot \sum_{k=k_0}^l \alpha_k^l \cdot V_k^l$ 
11       $h^l \leftarrow h^l + \alpha \cdot \text{RMSNORM}(O^l)$ ; // Refine current states
11 return  $h^L$ 

```

$$\begin{cases} \alpha^l = \text{diag}\left(\text{softmax}\left(\frac{q^l \cdot (K^l)^\top}{\sqrt{d'}}\right)\right) \\ O^l = W_{\text{out}} \cdot \sum_{k=k_0}^l \alpha_k^l \cdot V_k^l, \end{cases} \quad (8)$$

where α^l denotes the attention weights, and W_{out} projects the attention output from the latent dimension d' back to the original hidden dimension d . This design enables the attention mechanism to be performed in the latent space, efficiently reducing computational cost. The diagonal-only formulation ensures that each token aggregates information vertically across layers without interacting with other token positions.

Notably, the CLA module is parameter-shared across the whole network to reduce the introduced parameters and enhance the training efficiency. The detailed algorithm is shown in Algorithm 1.

4. Experiments

4.1. Experimental Setup

Models and Baselines. We implement our ICLA on two popular LVLMs—LLaVA1.5-7B and Qwen2.5-VL-7B—for comprehensive evaluation. We compare our ICLA with several strong hallucination mitigation baselines. Vanilla serves as the base model (LLaVA1.5-7B [25])

Model	LLaVA1.5-7B			Qwen2.5-VL-7B		
Method	MME	LLaVA-Bench	MMMU	MME	LLaVA-Bench	MMMU
Vanilla	1484	59.6	35.3	1689	87.0	67.5
DoLA	1485	60.5	35.7	1403	66.2	60.8
VCD	1469	60.6	35.8	1689	88.7	68.3
DeCo	1456	57.0	33.9	1681	86.8	62.5
POVID	1483	60.2	35.3	-	-	-
VDD	1484	59.4	34.9	1689	87.2	65.8
DAMO	1495	57.7	34.4	1681	87.4	65.8
<i>ICLA (Ours)</i>	1499	61.9	35.9	1711	90.2	69.2

Table 1. Experimental results on MME (total perception score), LLaVA-Bench (overall accuracy), and MMMU (accuracy) for LLaVA1.5-7B and Qwen2.5-VL-7B. The best results are highlighted in **bold** with light blue shading.

or Qwen2.5-VL-7B [2]). VCD [45] mitigates hallucinations by contrasting outputs from original and distorted visual inputs. VDD [45] extends VCD with post-hoc debiasing and debiased sampling. DoLA [5] contrasts logits across transformer layers to mitigate hallucinations. POVID [21] employs Direct Preference Optimization (DPO) to align the model and reduce hallucinations. DeCo [4] fuses information from selected preceding layers into the final decoding layer. DAMO [35] introduces momentum-based decoding to maintain inter-layer consistency and enhance factual grounding. For all experiments, the temperature is set to 0 for *greedy decoding* to ensure fair comparison.

Benchmarks and Metrics. We evaluate *ICLA* on four established hallucination benchmarks: POPE [23], MME [8], MMMU [43], and LLaVA-Bench [25]. POPE measures hallucination resistance on MSCOCO and A-OKVQA datasets under adversarial, random, and popular settings, reporting both accuracy and F1 scores. MME evaluates perception-related hallucinations, using the total perception score. MMMU tests multimodal reasoning ability with official accuracy. LLaVA-Bench adopts GPT-4o-based evaluation over perception, reasoning, and dialogue, providing both overall scores.

Training Details. We train *ICLA* using a lightweight tuning strategy with positive samples from the POVID training set, which consists of 17K examples randomly sampled from LLaVA-Instruct-150K. Notably, all data overlap with those used in the official LLaVA training, so no additional knowledge is introduced. All model parameters are frozen except for those in the *ICLA* module. The key hyperparameters are set as default: learning rate $lr = 2e - 5$, starting layer $k_0 = 16$, reduction ratio $r = 128$, and scaling factor $\alpha = 0.02$, training epochs $epoch = 3$.

4.2. Experimental Results

Results on LLaVA1.5-7B. As shown in Table 1 and Table 2, *ICLA* consistently outperforms all other baselines on

LLaVA1.5-7B. On the MME benchmark, *ICLA* achieves a 15-point improvement over the Vanilla LLaVA baseline and further surpasses contrastive decoding methods such as VCD and VDD by 30 and 15 points, respectively. On both LLaVA-Bench and MMMU, *ICLA* also attains the best performance. In particular, on LLaVA-Bench, *ICLA* reaches an accuracy of 61.9%, representing a 2.3% improvement over the Vanilla baseline. Compared to DAMO and DeCo, which also operate on hidden states during inference, *ICLA* further outperforms them by 4.9% and 4.2%, respectively. On the POPE benchmark, *ICLA* achieves the highest F1 and accuracy scores across both two datasets (MSCOCO and A-OKVQA) under all three settings, demonstrating that the flexible self-correction of *ICLA* is stronger than the curated methods for observed hallucination patterns.

Results on Qwen2.5-VL-7B. As shown in Table 1, *ICLA* also achieves outstanding results on Qwen2.5-VL-7B across the MME, LLaVA-Bench, and MMMU benchmarks. On the MME benchmark, we observe an interesting phenomenon: most baseline methods perform on par with or even worse than the Vanilla Qwen2.5-VL-7B. For example, only VCD and VDD achieve comparable scores to the baseline, while all other methods yield lower results, suggesting that these approaches may not generalize well to more advanced LLMs. In contrast, *ICLA* achieves a remarkable 22-point improvement over the Vanilla model, demonstrating both its effectiveness and strong adaptability. *ICLA* also attains the best performance on the MMMU benchmark, surpassing all baselines.

As shown in Table 2, *ICLA* further delivers strong results on the POPE benchmark. Specifically, it achieves the best F1 and accuracy across all three settings on the MSCOCO and A-OKVQA datasets. These results collectively demonstrate that *ICLA* is particularly effective and well-suited for more advanced LLMs such as Qwen2.5-VL-7B.

As shown in Table 3, we provide a fine-grained comparison across three tasks on LLaVA-Bench using Qwen2.5-

Setting	Method	LLaVA1.5-7B				Qwen2.5-VL-7B			
		MSCOCO		A-OKVQA		MSCOCO		A-OKVQA	
		F1	Acc	F1	Acc	F1	Acc	F1	Acc
Adversarial	Vanilla	81.76	79.77	76.12	69.37	80.72	83.40	80.73	79.53
	DoLA	81.69	79.73	76.22	69.53	77.44	80.63	80.91	76.57
	VCD	80.50	78.33	75.05	67.97	81.13	77.77	80.73	72.03
	DeCo	81.14	78.37	74.93	67.03	80.86	83.47	80.93	80.10
	POVID	81.88	80.03	76.18	69.47	-	-	-	-
	DAMO	81.65	79.53	75.96	68.97	80.84	83.47	81.09	80.30
	<i>ICLA (Ours)</i>	81.90	80.13	76.32	69.73	81.50	83.97	81.60	80.93
Popular	Vanilla	86.82	86.23	83.22	80.30	81.03	83.73	85.32	85.83
	DoLA	86.84	86.30	83.33	80.47	77.70	80.97	84.66	83.00
	VCD	84.80	83.97	81.02	77.43	81.02	77.67	85.48	74.37
	DeCo	85.90	84.73	81.39	77.47	81.24	83.90	85.45	86.20
	POVID	86.78	86.23	83.32	80.53	-	-	-	-
	DAMO	86.84	86.20	83.04	79.97	81.25	83.90	85.56	86.27
	<i>ICLA (Ours)</i>	86.91	86.43	83.39	80.57	81.92	84.37	86.37	87.07
Random	Vanilla	89.71	89.60	88.52	87.33	81.58	84.37	87.06	87.63
	DoLA	89.77	89.70	88.55	87.37	78.02	81.57	85.91	84.43
	VCD	87.60	87.37	86.52	85.00	81.64	79.17	87.86	80.77
	DeCo	89.29	88.83	86.53	84.67	81.78	84.50	87.27	88.10
	POVID	89.56	89.50	88.29	87.07	-	-	-	-
	DAMO	89.69	89.53	87.93	86.53	81.83	84.57	87.32	88.13
	<i>ICLA (Ours)</i>	89.95	89.93	88.80	87.70	82.59	85.10	88.28	89.03

Table 2. **Results on the POPE benchmark.** Comparison between **LLaVA1.5-7B** and **Qwen2.5-VL-7B**. We report F1 Score (%) and Accuracy (%) on the MSCOCO and A-OKVQA datasets under Adversarial, Popular, and Random settings. The best results are highlighted in **bold blue**.

Method	Vanilla	DoLA	VCD	DeCo	VDD	DAMO	ICLA (Ours)
Complex Reasoning (%)	95.8	66.5	98.6	95.2	94.8	96.3	93.3
Conversation (%)	82.4	65.0	86.1	83.7	85.0	82.0	89.4
Detail Description (%)	76.0	66.9	74.4	75.8	76.4	77.7	85.5
All (%)	87.0	66.2	88.7	86.8	87.2	87.4	90.2

Table 3. Comparison of LLaVA-Bench performance for various baselines with backbone Qwen2.5-VL-7B. The best results are highlighted in **bold blue**.

7B-VL as the backbone to demonstrate the effectiveness of ICLA in generalized hallucination mitigation. From an overall perspective, most baselines achieve performance comparable to vanilla Qwen2.5-VL-7B (87.0%), whereas ICLA unexpectedly reaches 90.2%, yielding a substantial 3.2% improvement. Examining the task-level results, ICLA

delivers particularly strong gains on Conversation and Detailed Description, with improvements of 7% and 9.5%, respectively. These significant increases further demonstrate the robustness and general applicability of our method across diverse hallucination scenarios.

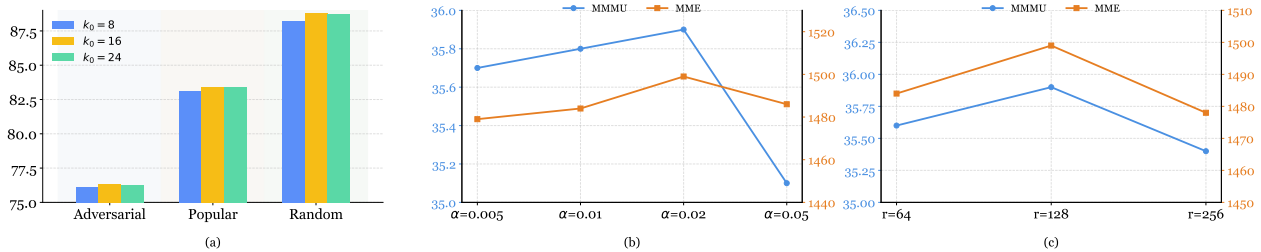


Figure 3. (a) Ablation results for starting layer k_0 on POPE benchmark. (b) Ablation results for reduction ratio r on MMMU and MME benchmarks; (c) Ablation results on scaling factor α on MMMU and MME benchmarks.

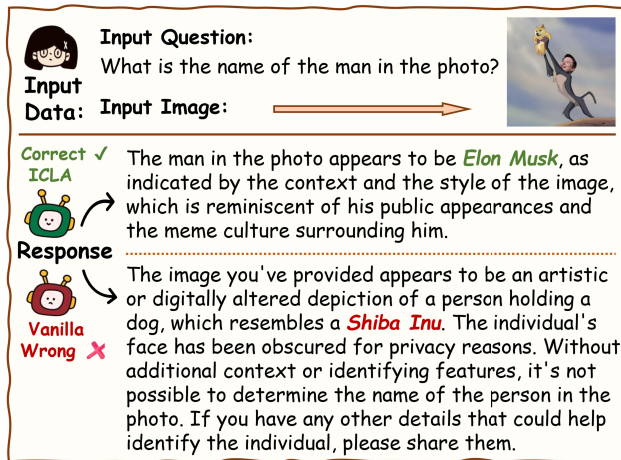


Figure 4. Case study comparing *Vanilla* and *ICLA* based on Qwen2.5-VL-7B. The example is sampled from LLaVA-Bench.

4.3. Case Study

We present a case study to qualitatively illustrate the effectiveness of *ICLA* in mitigating hallucinations. The underlying model is Qwen2.5-VL-7B, and the example is sampled from LLaVA-Bench. As shown in Figure 4, when given the textual prompt “What is the name of the man in the photo?” along with an image showing Elon Musk holding a dog—but with the body replaced by that of an animal—the scene introduces significant confusion. In this case, the vanilla Qwen model incorrectly identifies the man in the photo as “Shiba Inu.” In contrast, *ICLA*, correctly recognizes the person as Elon Musk despite the misleading visual cues. This demonstrates that *ICLA* can effectively and systematically reduce hallucinations in multimodal reasoning.

4.4. Ablation Studies

Hyperparameter Studies. To evaluate the robustness and generalizability of *ICLA*, we conduct comprehensive ablation studies on the POPE, MME, and MMMU benchmarks using LLaVA1.5-7B. In each experiment, we vary a single

key hyperparameter while keeping the others fixed at their default values. Specifically, we analyze the effects of the starting layer k_0 , the reduction ratio r , and the scaling factor α . As shown in Figure 3(a), (b), and (c), the default settings yield the best performance. Moreover, the results exhibit only minor fluctuations as the parameters vary, demonstrating that *ICLA* is robust and relatively insensitive to hyperparameter changes.

ICLA in Each Layer. To further assess the effectiveness of *ICLA*, we conduct ablation studies comparing different variants of the mechanism. The first variant applies layer attention only at the final layer, where the final hidden state serves as the query to retrieve information from all preceding layers. The second variant employs random aggregation, in which skip connections are added randomly, allowing certain layers to receive information from previous layers in a non-deterministic manner. As shown in Table 4, the full *ICLA* consistently outperforms all other variants, further demonstrating the importance of structured, layer-wise attention in effectively integrating cross-layer information and mitigating hallucinations.

Method	Random		Adversarial	
	F1	Acc	F1	Acc
Vanilla	88.52	87.33	76.12	69.37
ICLA (Last)	88.29	87.40	76.18	69.47
Random Agg.	88.55	87.37	76.18	69.47
ICLA	88.80	87.70	76.32	69.73

Table 4. Comparison of different *ICLA* variants on the POPE benchmark (A-OKVQA dataset) using LLaVA1.5-7B. *Random Add.* denotes the Random Aggregation.

4.5. Analysis and Discussion

Training and Inference Efficiency. *ICLA* is highly training-efficient. Training is performed on two RTX 4090 GPUs for 3 epochs with a learning rate of $2e-5$ for each

model, taking approximately 3 hours. As detailed in the Appendix, ICLA introduces only 277K and 105K additional parameters for LLaVA1.5-7B and Qwen2.5-VL-7B, respectively. This is because the parameters for each CLA module are shared within the whole network and we operate the cross-layer attention in the latent hidden space. The average inference-time computational overhead under different token length is also minimal, accounting for only 0.37% and 0.07% of the total computation in LLaVA and Qwen2.5-VL-7B, respectively.

Layer Attention Pattern Analysis. As mentioned earlier, there is no consistent hallucination trend across more advanced models. To address this, we design a more scalable architecture that enables each hidden state to adaptively select and integrate information from previous layers for self-correcting, thereby mitigating hallucination. While this approach proves effective, in this section we try to interpret and uncover deeper insights into the underlying attention dynamics.

We analyze the layer-wise attention behavior on samples from the POPE benchmark (MSCOCO dataset), where the vanilla Qwen2.5-VL-7B initially produces incorrect answers but ICLA successfully corrects them. For each layer l (as the query), we record and visualize the average attention weights over the preceding layers from k_0 to l .

As shown in Figure 5, we identify two prominent regions of attention concentration in Qwen2.5-VL-7B. First, layers 19–21 exhibit strong attention, suggesting that intermediate layers play a crucial role in reasoning. This indicates that emphasizing these representations may contribute to mitigating hallucinations. Second, the later layers, particularly 24–25, also show high cross-layer retrieval, implying that both intermediate and deeper layers jointly facilitate reasoning and self-correction.

In contrast, three regions—layers 16–18, 22–23, and, surprisingly, 26–28—receive almost no attention. This suggests that the model largely ignores information from these layers during self-correction. Notably, the final layer (28-th), responsible for next-token prediction, primarily retrieves information from layers 21, 24, and 25 when making decisions. This observation further supports the idea that referencing earlier informative layers, rather than relying solely on the final representations, enhances the model’s ability to refine its outputs.

Interestingly, these attended and unattended regions alternate throughout the network, forming an interleaved pattern. Such alternation reflects a dynamic balance between information consolidation and abstraction across depth, highlighting that not all layers contribute equally to reasoning or correction.

Broader Applicability. We further conduct a similar layer-wise attention analysis on LLaVA-1.5-7B to exam-

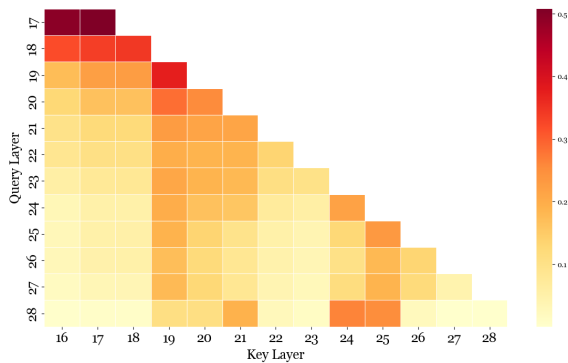


Figure 5. Visualization of average attention weights in ICLA using Qwen for selected samples

ine whether the observed patterns generalize across models. Interestingly, the attention distribution in LLaVA1.5-7B differs entirely from that of Qwen2.5-VL-7B, showing no consistent concentration regions or interleaved structures. This discrepancy indicates that the curated hallucination mitigation strategies specifically designed for LLaVA may not directly transfer to Qwen2.5-VL-7B (As our preliminary experiments in Figure 1). Consequently, our proposed method is not only effective for alleviating hallucinations but also serves as a general analytical tool for identifying key layers in more advanced models where traditional hallucination patterns become less observable. From the perspective of attention-weight distribution, our approach provides a principled way to investigate how higher-level models internally allocate reasoning focus across depth.

5. Conclusion

In this paper, we reveal that previously observed hallucination patterns and their corresponding mitigation methods are no longer effective for more advanced LVLMS. With the use of higher-quality data and more sophisticated training strategies, no consistent hallucination trends can be observed in these models. To address this limitation, we propose ICLA, an internal self-correction mechanism that leverages layer-wise attention to dynamically retrieve and refine information from preceding hidden states during generation. Extensive experiments across multiple benchmarks and models, including LLaVA1.5-7B and Qwen2.5-VL-7B, demonstrate that ICLA consistently outperforms other strong baselines, effectively mitigating hallucinations. Our results highlight the potential of adaptive, cross-layer mechanisms for improving the reliability of advanced LVLMS, even in scenarios where no clear hallucination patterns are observable.

References

- [1] Jean-Baptiste Alayrac, Jeff Donahue, Pierre Luc, Antoine Miech, Ishan Barr, Yossi Hasson, Smaine Milani, Sebastian Borgeaud, Arthur Mensch, Serkan Cabi, et al. Flamingo: a visual language model for few-shot learning. *arXiv preprint arXiv:2204.14198*, 2022. 1
- [2] Shuai Bai, Keqin Chen, Xuejing Liu, Jialin Wang, Wenbin Ge, Sibao Song, Kai Dang, Peng Wang, Shijie Wang, Jun Tang, et al. Qwen2. 5-vl technical report. *arXiv preprint arXiv:2502.13923*, 2025. 2, 5
- [3] Xinyun Chen, Renat Aksitov, Uri Alon, Jie Ren, Kefan Xiao, Pengcheng Yin, Sushant Prakash, Charles Sutton, Xuezhi Wang, and Denny Zhou. Universal self-consistency for large language model generation. *arXiv preprint arXiv:2311.17311*, 2023. 1
- [4] Yuxian Chen, Xiaolong Han, Yichong Zhang, and Minlie Tan. Mllm can see? dynamic correction decoding for hallucination mitigation. *arXiv preprint arXiv:2410.11779*, 2024. 1, 2, 3, 5
- [5] Yung-Sung Chuang, Yujia Xie, Hongyin Luo, Yoon Kim, James Glass, and Pengcheng He. Dola: Decoding by contrasting layers improves factuality in large language models. *arXiv preprint arXiv:2309.03883*, 2023. 1, 2, 5
- [6] William Claster, Suhas KM, and Dhairya Gundecha. Adaptive integrated layered attention (aila). *arXiv preprint arXiv:2503.22742*, 2025. 3
- [7] Yanwen Fang, Yuxi Cai, Jintai Chen, Jingyu Zhao, Guangjian Tian, and Guodong Li. Cross-layer retrospective retrieving via layer attention. *arXiv preprint arXiv:2302.03985*, 2023. 3
- [8] Chaoyou Fu, Peixian Chen, Yunhang Shen, Yulei Qin, Mengdan Zhang, Xu Lin, Jinrui Yang, Xiawu Zheng, Ke Li, Xing Sun, Yunsheng Wu, and Rongrong Ji. MME: A comprehensive evaluation benchmark for multimodal large language models. *arXiv preprint arXiv:2306.13394*, 2023. 1, 5
- [9] Zorik Gekhman, Gal Yona, Roei Aharoni, Matan Eyal, Amir Feder, Roi Reichart, and Jonathan Herzig. Does fine-tuning llms on new knowledge encourage hallucinations? *arXiv preprint arXiv:2405.05904*, 2024. 2
- [10] Yash Goyal, Tejas Khot, Douglas Summers-Stay, Dhruv Batra, and Devi Parikh. Making the v in vqa matter: Elevating the role of image understanding in visual question answering. In *Proceedings of the IEEE conference on computer vision and pattern recognition*, pages 6904–6913, 2017. 1
- [11] Tianrui Guan, Fuxiao Liu, Xiyang Wu, Ruiqi Xian, Zongxia Li, Xiaoyu Liu, Xijun Wang, Lichang Chen, Furong Huang, Yaser Yacoob, et al. Hallusionbench: an advanced diagnostic suite for entangled language hallucination and visual illusion in large vision-language models. In *Proceedings of the IEEE/CVF Conference on Computer Vision and Pattern Recognition*, pages 14375–14385, 2024. 2
- [12] Yudong Han, Liqiang Nie, Jianhua Yin, Jianlong Wu, and Yan Yan. Visual perturbation-aware collaborative learning for overcoming the language prior problem. *arXiv preprint arXiv:2207.11850*, 2022. 2
- [13] Minda Hu, Bowei He, Yufei Wang, Liangyou Li, Chen Ma, and Irwin King. Mitigating large language model hallucination with faithful finetuning. *arXiv preprint arXiv:2406.11267*, 2024. 2
- [14] Zhongzhan Huang, Senwei Liang, Mingfu Liang, and Haizhao Yang. Dianet: Dense-and-implicit attention network. In *Proceedings of the AAAI conference on artificial intelligence*, pages 4206–4214, 2020. 3, 4
- [15] Fushuo Huo, Wenchao Xu, Zhong Zhang, Haozhao Wang, Zhicheng Chen, and Peilin Zhao. Self-introspective decoding: Alleviating hallucinations for large vision-language models. *arXiv preprint arXiv:2408.02032*, 2024. 3
- [16] Prannay Kaul, Zhizhong Li, Hao Yang, Yonatan Dukler, Ashwin Swaminathan, CJ Taylor, and Stefano Soatto. Throne: An object-based hallucination benchmark for the free-form generations of large vision-language models. In *Proceedings of the IEEE/CVF Conference on Computer Vision and Pattern Recognition*, pages 27228–27238, 2024. 2
- [17] Aviral Kumar, Vincent Zhuang, Rishabh Agarwal, Yi Su, John D Co-Reyes, Avi Singh, Kate Baumli, Shariq Iqbal, Colton Bishop, Rebecca Roelofs, et al. Training language models to self-correct via reinforcement learning. *arXiv preprint arXiv:2409.12917*, 2024. 1
- [18] Yi-Lun Lee, Yi-Hsuan Tsai, and Wei-Chen Chiu. Delve into visual contrastive decoding for hallucination mitigation of large vision-language models. *arXiv preprint arXiv:2412.06775*, 2024. 1, 3
- [19] Junnan Li, Kailan Li, Silvio Savarese, and Juan Carlos Niebles. Blip-2: Bootstrapping language-image pre-training with frozen image encoders and large language models. *arXiv preprint arXiv:2301.12597*, 2023. 1
- [20] Shuo Li, Minghao Li, Bing Li, and Jie Xu. Opera: Alleviating hallucination in multi-modal large language models via over-trust penalty and retrospection-allocation. *arXiv preprint arXiv:2311.17911*, 2023. 1
- [21] Shuo Li, Xiaoxuan Zheng, Jie Xu, Bing Li, and Jing Lin. Aligning modalities in vision large language models via preference fine-tuning. *arXiv preprint arXiv:2402.11411*, 2024. 1, 2, 5
- [22] Xiang Lisa Li, Ari Holtzman, Daniel Fried, Percy Liang, Jason Eisner, Tatsunori Hashimoto, Luke Zettlemoyer, and Mike Lewis. Contrastive decoding: Open-ended text generation as optimization. *arXiv preprint arXiv:2210.15097*, 2022. 2
- [23] Yifan Li, Yifan Du, Kun Zhou, Jinpeng Wang, Wayne Xin Zhao, and Ji-Rong Wen. Evaluating object hallucination in large vision-language models. *arXiv preprint arXiv:2305.10355*, 2023. 5
- [24] Tsung-Yi Lin, Michael Maire, Serge Belongie, James Hays, Pietro Perona, Deva Ramanan, Piotr Dollár, and C Lawrence Zitnick. Microsoft coco: Common objects in context. In *Computer vision—ECCV 2014: 13th European conference, zurich, Switzerland, September 6–12, 2014, proceedings, part v 13*, pages 740–755. Springer, 2014. 1
- [25] Haotian Liu, Chunyuan Li, Qingyang Wu, and Yong Jae Lee. Visual instruction tuning. *Advances in Neural Information Processing Systems*, 36:34892–34916, 2023. 1, 4, 5

- [26] Xinyu Lyu, Beita Chen, Lianli Gao, Hengtao Shen, and Jingkuan Song. Alleviating hallucinations in large vision-language models through hallucination-induced optimization. *Advances in Neural Information Processing Systems*, 37:122811–122832, 2024. 3
- [27] Avshalom Manevich and Reut Tsarfaty. Mitigating hallucinations in large vision-language models (lvm) via language-contrastive decoding (lcd). *arXiv preprint arXiv:2408.04664*, 2024. 1, 3
- [28] OpenAI. Gpt-4 technical report. *arXiv preprint arXiv:2303.08774*, 2023. 1
- [29] Yeji Park, Deokyeong Lee, Junsuk Choe, and Buru Chang. Convis: Contrastive decoding with hallucination visualization for mitigating hallucinations in multimodal large language models. In *Proceedings of the AAAI Conference on Artificial Intelligence*, pages 6434–6442, 2025. 1, 3
- [30] Rafael Rafailov, Archit Sharma, Eric Mitchell, Christopher D Manning, Stefano Ermon, and Chelsea Finn. Direct preference optimization: Your language model is secretly a reward model. *Advances in neural information processing systems*, 36:53728–53741, 2023. 2
- [31] Rico Sennrich, Jannis Vamvas, and Alireza Mohammadshahi. Mitigating hallucinations and off-target machine translation with source-contrastive and language-contrastive decoding. *arXiv preprint arXiv:2309.07098*, 2023. 2
- [32] Wei Suo, Lijun Zhang, Mengyang Sun, Lin Yuanbo Wu, Peng Wang, and Yanning Zhang. Octopus: Alleviating hallucination via dynamic contrastive decoding. In *Proceedings of the Computer Vision and Pattern Recognition Conference*, pages 29904–29914, 2025. 1, 3
- [33] Kai Tang, Jinhao You, Xiuqi Ge, Hanze Li, Yichen Guo, and Xiande Huang. Mitigating hallucinations via inter-layer consistency aggregation in large vision-language models. *arXiv preprint arXiv:2505.12343*, 2025. 1, 2, 3, 4
- [34] Kaishen Wang, Xun Xia, Jian Liu, Zhang Yi, and Tao He. Strengthening layer interaction via dynamic layer attention. *arXiv preprint arXiv:2406.13392*, 2024. 3, 4
- [35] Kaishen Wang, Hengrui Gu, Meijun Gao, and Kaixiong Zhou. Damo: Decoding by accumulating activations momentum for mitigating hallucinations in vision-language models. In *The Thirteenth International Conference on Learning Representations*, 2025. 1, 2, 3, 4, 5
- [36] Liu Wang, Xin Zheng, Shuo Li, Jie Xu, and Lei Lin. Rlhfv: Towards trustworthy mllms via behavior alignment from fine-grained correctional human feedback. *arXiv preprint arXiv:2312.00849*, 2023. 1, 2
- [37] Lei Wang, Jiabang He, Shenshen Li, Ning Liu, and Ee-Peng Lim. Mitigating fine-grained hallucination by fine-tuning large vision-language models with caption rewrites. In *International Conference on Multimedia Modeling*, pages 32–45. Springer, 2024. 1, 2, 3
- [38] Xuezhi Wang, Jason Wei, Dale Schuurmans, Quoc Le, Ed Chi, Sharan Narang, Aakanksha Chowdhery, and Denny Zhou. Self-consistency improves chain of thought reasoning in language models. *arXiv preprint arXiv:2203.11171*, 2022. 1
- [39] Zhenyu Wu, Qingkai Zeng, Zhihan Zhang, Zhaoxuan Tan, Chao Shen, and Meng Jiang. Large language models can self-correct with key condition verification. *arXiv preprint arXiv:2405.14092*, 2024. 1
- [40] Chen Xu, Yuchen Liu, and Lei Lin. Alleviating hallucinations in large vision-language models through hallucination-induced optimization. *arXiv preprint arXiv:2405.15356*, 2024. 2
- [41] Le Yu, Kaishen Wang, Jianlong Xiong, Yue Cao, and Tao He. Hallurnn: Mitigating hallucinations via recurrent cross-layer reasoning in large vision-language models. *arXiv preprint arXiv:2506.17587*, 2025. 1, 2, 3, 4
- [42] Weihao Yu, Zhengyuan Yang, Linjie Li, Jianfeng Wang, Kevin Lin, Zicheng Liu, Xinchao Wang, and Lijuan Wang. Mm-vet: Evaluating large multimodal models for integrated capabilities. *arXiv preprint arXiv:2308.02490*, 2023. 1
- [43] Xiang Yue, Yuansheng Ni, Kai Zhang, Tianyu Zheng, Ruoqi Liu, Ge Zhang, Samuel Stevens, Dongfu Jiang, Weiming Ren, Yuxuan Sun, et al. Mmmu: A massive multi-discipline multimodal understanding and reasoning benchmark for expert agi. In *Proceedings of the IEEE/CVF Conference on Computer Vision and Pattern Recognition*, pages 9556–9567, 2024. 5
- [44] Ce Zhang, Zifu Wan, Zhehan Kan, Martin Q Ma, Simon Stepputtis, Deva Ramanan, Russ Salakhutdinov, Louis-Philippe Morency, Katia Sycara, and Yaqi Xie. Self-correcting decoding with generative feedback for mitigating hallucinations in large vision-language models. *arXiv preprint arXiv:2502.06130*, 2025. 3
- [45] Rui Zhang, Yuan Wang, Xiao Li, Xiaodong Zhang, and Yang Zhao. Mitigating object hallucinations in large vision-language models through visual contrastive decoding. *arXiv preprint arXiv:2311.16922*, 2023. 1, 2, 5
- [46] Yi-Fan Zhang, Weichen Yu, Qingsong Wen, Xue Wang, Zhang Zhang, Liang Wang, Rong Jin, and Tieniu Tan. Debiasing multimodal large language models. *arXiv preprint arXiv:2403.05262*, 2024.
- [47] Yihe Zhou, Huikai Lin, Zhixiang Xie, Qicheng Wang, and Yifan Liu. Ibd: Alleviating hallucinations in large vision-language models via image-biased decoding. *arXiv preprint arXiv:2402.18476*, 2024. 1, 2, 3
- [48] Ding Zhu, Xu Lin, Yu Hu, and Zhiqiang Lin. Minigt-4: Enhancing vision-language understanding with advanced large language models. *arXiv preprint arXiv:2304.10592*, 2023. 1

Appendix

A. Detailed Results

We present the detailed results shown in Table 1. Experimental results for MME evaluated on Qwen2.5-VL-7B are shown in Table 5, results for MMMU evaluated on Qwen2.5-VL-7B are shown in Table 6, results for LLaVA-Bench evaluated on LLaVA1.5-7B are shown in Table 7.

B. Further Evaluation

To further evaluate the effectiveness of ICLA, we also apply ICLA in more advanced model, Qwen3-VL-8B. We compare ICLA with various decoding strategies on MME, LLaVA-Bench, and MMMU benchmarks. As shown in Table 8, ICLA consistently outperforms all other baselines across these three benchmarks, further demonstrating the effectiveness of ICLA in mitigating hallucinations in more advanced model. We believe the further experiments prove that ICLA is more adaptive and scalable for mitigating hallucination in LLMs.

C. Additional Attention Pattern

In addition to the attention pattern analysis for Qwen2.5-VL-7B in the main paper, we further present the attention pattern for LLaVA1.5-7B. As shown in Figure 6, the attention pattern in LLaVA shows that only intermediate layers are frequently retrieved, showcasing totally different attention pattern from Qwen2.5-VL-7B. This observation is consistent with previous researches that intermediate layers contribute more to hallucination mitigation in LLaVA. We further argue the broader applicability for ICLA, which provides a principled way to investigate how higher-level models internally allocate reasoning focus across depth.

D. Efficiency of ICLA

We further provide the efficiency of ICLA. As shown in Table 9 and Table 10, we present the extra FLOPs and the introduced parameters for ICLA in LLaVA1.5-7B and Qwen2.5-VL-7B, respectively. The results show that ICLA introduces small number of computation overhead and parameters, demonstrating the efficiency of ICLA.

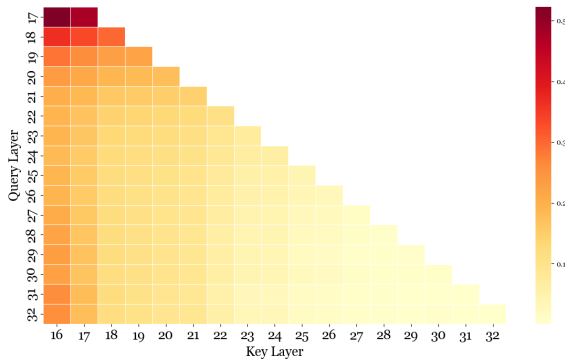


Figure 6. Visualization of average attention weights in ICLA using LLaVA1.5-7B for selected samples

Method	OCR	Artwork	Celebrity	Color	Count	Existence	Landmark	Position	Posters	Scene	Total
Vanilla	181	138	157	194	154	199	184	159	169	154	1689
DoLA	165	115	87	184	118	174	121	154	146	139	1403
VCD	181	138	157	194	154	199	184	159	169	154	1689
DeCo	181	138	153	194	154	199	181	159	168	154	1681
VDD	181	138	157	194	154	199	184	159	169	154	1689
DAMO	181	138	153	194	154	199	181	159	168	154	1681
ICLA (Ours)	179	149	159	194	154	199	189	159	173	156	1711

Table 5. Comparison on the MME benchmark (Perception) across various baselines with backbone Qwen2.5-VL-7B. The best results are highlighted in **bold**.

Method	Vanilla	DoLa	VCD	DeCo	VDD	DAMO	ICLA (Ours)
Overall Accuracy(%)	67.5	60.8	68.3	62.5	65.8	65.8	69.2

Table 6. Comparison on overall accuracy of the MMMU benchmark across various baselines with backbone Qwen2.5-VL-7B. The best results are highlighted in **bold**.

Method	Vanilla	DoLa	VCD	DeCo	POVID	VDD	DAMO	ICLA (Ours)
Complex reasoning (%)	72.1	70.5	70.7	66.8	69.4	71.9	65.1	70.4
Conversation (%)	50.6	53.7	55.0	52.7	55.0	52.3	55.0	59.6
Detail description (%)	48.8	50.0	49.3	45.0	50.4	45.7	48.0	50.0
All (%)	59.6	60.5	60.6	57.0	60.2	59.4	57.7	61.9

Table 7. Comparison of LLaVA-Bench performance for various baselines. The best results are highlighted in **bold**.

Method	MME	LLaVA-Bench	MMMU
Vanilla	1726	98.8	57.1
DoLA	1705	99.8	58.0
VCD	1726	106.7	57.1
DeCo	1734	60.6	57.2
VDD	1720	106.3	56.5
DAMO	1704	102.8	56.9
ICLA (Ours)	1740	106.8	58.3

Table 8. Experimental results on MME (total perception score), LLaVA-Bench (overall accuracy), and MMMU (accuracy) for Qwen3-VL-8B. The best results are highlighted in **bold**.

Token Length	Total FLOPs (TFLOPs)	ICLA FLOPs (GFLOPs)	Overhead (%)	Params Added
128	5.12	18.8	0.37	
256	10.29	37.8	0.37	277K
512	13.86	50.6	0.37	

Table 9. Computation overhead of ICLA compared to vanilla LLaVA1.5-7B under different token lengths.

Token Length	Total FLOPs (TFLOPs)	ICLA FLOPs (GFLOPs)	Overhead (%)	Params Added
128	2.12	1.48	0.07	
256	4.36	2.98	0.07	105K
512	7.99	5.94	0.07	

Table 10. Computation overhead of ICLA compared to vanilla Qwen2.5-VL-7B under different token lengths.